

Analysis of the Micropipette Experiment for Thin Biological Samples

Thomas BOUDOU¹, Philippe TRACQUI¹, Gérard FINET² & Jacques OHAYON¹

¹Laboratoire TIMC-IMAG, Equipe DynaCell
CNRS, UMR 5525, IN³S

38706 La Tronche Cedex - FRANCE

²Hôpital Cardiologique, Lyon Montchat, 69394 Lyon Cedex 03, FRANCE

Abstract: Even if micropipette experiment is a quite widely used micromanipulation technique, the derived Young's modulus of the probe tissue can be overestimated if thin samples are used. In this paper finite element models were used to examine the influence of sample thickness h on the mechanical response. Considering the assumptions of quasi-incompressible elastic material undergoing small strains, our numerical results show that below a critical value of h , the thickness of the sample becomes a relevant parameter and must be taken into account for accurately determining the mechanical properties of the tissue. This study provides a framework in which finite element modeling of biological tissue rheology would help to decrease the bias and thus the dispersion of elastic modulus estimated from micropipette experiments.

Key-Words: Mechanical model - Elasticity - Finite element method - Micropipette

1 Introduction

Understanding how a biological material interacts with its environment requires the knowledge of its mechanical properties. The micropipette aspiration technique is a widely used experimental method which has been extensively applied in recent years to measure the elasticity of cell cytoskeleton [1, 2, 3, 4], cell nucleus [5] as well as aortic tissue [6]. The effects of the internal pipette radius and its thickness on the mechanical sample response have been largely studied [3]. More recently, it has been shown that the initial curvature of the aspirated surface sample affects significantly the mechanical response [4]. Nevertheless, while quantification of the tissue elastic modulus is a central issue of this experimental approach, the proposed relationships between imposed suction pressure and measured aspirated length can not be used for thin biological samples. In the present work, we extend the work of Theret et al. [3] in order to - (i) correct previous analytical expression obtained for a semi-infinite homogeneous medium (or half-space model) by including a geometrical function which account for the thickness of the sample, and to - (ii) establish critical values of the sample height below which such correcting coefficient are necessary.

2 Finite Element Model

Computations of the aspirated length induced by increasing the value of the micropipette negative pressure were performed using Ansys 8.0 software

(Ansys 8.0 software, Ansys Inc., Connsburg, Pennsylvania, USA).

2.1 Geometry

The tissue is represented by a thick circular slice of radius a and thickness h . The pipette is modeled by a rigid hollow cylinder of internal and external radii R_i and R_e , respectively. Taking advantage of the axisymmetry conditions of revolution, we simplify the mechanical study to a two-dimensional structural analysis (Fig. 1).

2.2 Material properties and mathematical formulation

The tissue is assumed to be an isotropic and incompressible elastic medium, with Young's modulus E . Considering only small deformation of the homogeneous tissue sample, the governing equations in the absence of body force are given by

$$\text{div}\boldsymbol{\sigma}=\mathbf{0}, \boldsymbol{\sigma}=-p\mathbf{I}+2G\boldsymbol{\varepsilon}, 2\boldsymbol{\varepsilon}=\text{gradu}+(\text{gradu})^T, \text{div}\mathbf{u}=\mathbf{0} \quad (1)$$

where $\boldsymbol{\sigma}$ and $\boldsymbol{\varepsilon}$ are the stress and strain tensors, \mathbf{I} is the identity matrix, \mathbf{u} is the displacement vector, p is the Lagrange multiplier resulting from material incompressibility, and G is the material shear modulus (related to the Young's modulus E by the relationship $G=E/3$).

2.3 Boundary and contact Conditions

We meshed the tissue with approximately 4,500 high-order eight nodes elements and we especially

concentrated the number of elements in the neighborhood of the aspirated region (Fig.1).

The contact lines between the pipette and the tissue are particularly finely meshed with specific contact elements in order to allow sliding of the aspirated tissue on the tip of the micropipette.

The following displacement conditions were imposed on the tissue boundaries: (i) Zero displacement, modeling full tissue attachment to the base, was imposed to the tissue side in contact with the rigid substrate, (ii) zero normal displacement condition was imposed on the tissue section belonging to the axis of symmetry, (iii) free boundary conditions were assumed for all the other sample sides, (iv) zero displacement was imposed to all the surface of the micropipette.

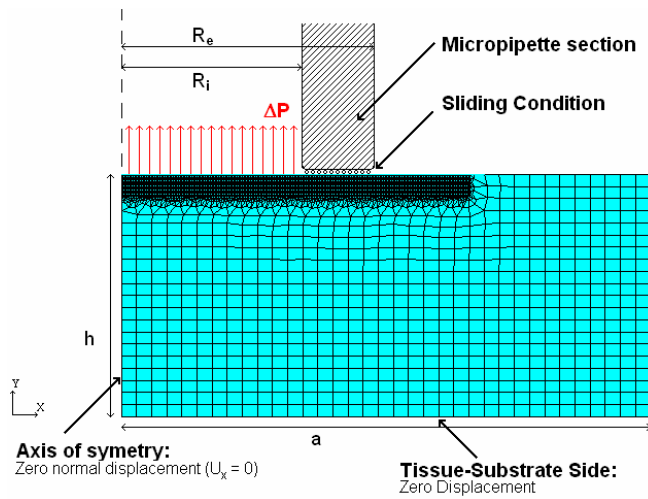


Fig.1: Finite element mesh, boundary conditions and geometrical parameters.

3 Results

3.1 Background for the calculation of tissue Young's modulus

In the case of a semi-infinite sample (i.e. when a and h tend to infinity) and under the assumptions of linear elasticity and incompressible medium, the displacement field solution of Eqs.(1) has been found by Theret et al. [3]. The resulting relationship between the applied negative pressure ΔP and the associated aspirated length U_y , depends on tissue Young's modulus E , pipette inner diameter R_i and wall function $\Phi(\eta)$ [3]:

$$U_y^{h=\infty} = \frac{3\Delta P}{2\pi E} R_i \Phi(\eta) \quad (2)$$

where $\eta = (R_e - R_i)/R_i$ and $\Phi(\eta) \approx 2$ for realistic values of η ranging from 0.4 to 0.6. In real micropipette

experiments, variations of sample thickness can significantly modify its mechanical response. It is thus of importance to study the sensitivity of the aspirated tissue length U_y to modifications of the geometrical parameters h relatively to the pipette inner radius R_i .

3.2 Model validation

An estimation of the numerical error is performed by comparison of the computed solution with the previous analytical solution derived by Theret et al. [3]. We checked that the computed values (obtained with $h_\infty = 40 \mu\text{m}$ and $a_\infty = 40 \mu\text{m}$) agreed within 4 % with the corresponding theoretical values.

3.3 Spatial distribution of effective strains with variation of sample thickness

Figure 2 highlights the effect of decreasing tissue thickness on the spatial distributions of the effective strain within the medium when h varies ($h=1\mu\text{m}$ and $h=4\mu\text{m}$). The effective strain is defined as $\varepsilon_{\text{eff}} = (2e_{ij}e_{ij}/3)^{0.5}$, where e_{ij} are the components of the deviatoric strain tensor. In these two cases, for given micropipette geometries, mechanical properties of the tissue and imposed internal pressure ($R_i = 1 \mu\text{m}$, $R_e = 1.4 \mu\text{m}$, $E = 1 \text{ kPa}$, and $\Delta P = 40 \text{ Pa}$), the resulting computed aspirated tissue length are $U_y = 1.92 \times 10^{-2} \mu\text{m}$ and $U_y = 3.92 \times 10^{-2} \mu\text{m}$, respectively.

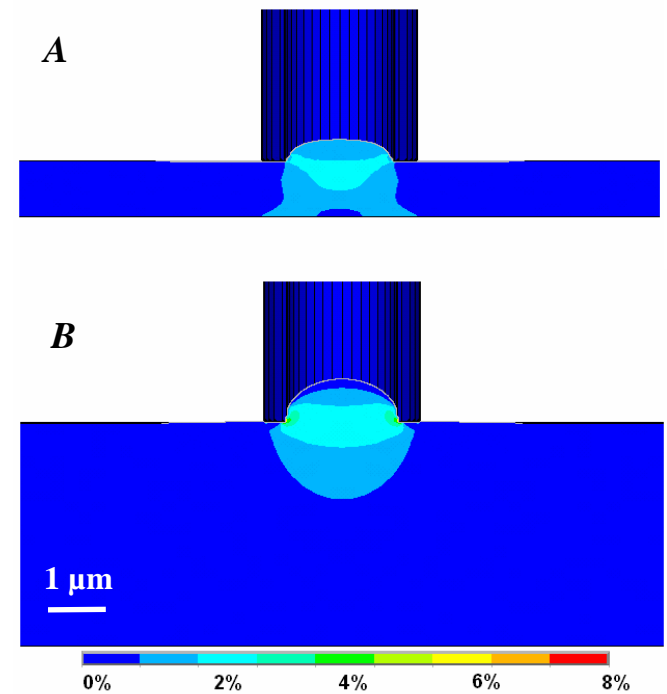


Fig.2: 3D color maps showing the tissue deformed shapes and the spatial distributions of the effective strain ε_{eff} . **A**) $h = 1 \mu\text{m}$ - **B**) $h = 4 \mu\text{m}$. Displacement scale has been multiplied by 20 to highlight the simulation results.

3.4 Nonlinear corrections of the half-space model

In order to introduce the thickness effect and to correct the Theret et al.'s solution given by Eq.(2), we used a finite element model to extensively compute and analyze the tissue response to applied negative pressure ΔP for a large set (200 cases) of pipettes and sample thicknesses in the range: $1\mu\text{m} \leq R_i \leq 10\mu\text{m}$, $2\mu\text{m} \leq h \leq 60\mu\text{m}$ and $0.4 \leq \eta \leq 0.6$. To avoid edge effects, the tissue width a is approximately 5 times larger than the inner radius of the pipette.

On Fig. 3 we compare the simulated results with the analytical half-space model solution given by Eq.(2). Interestingly, our computations allow us to correct the previous solution $U_y^{h=\infty}$ by introducing a new geometrical function β which depends only of the normalized thickness sample h/R_i :

$$U_y = \beta(h/R_i) U_y^{h=\infty} \quad (3)$$

As expected, the values of the geometrical function β satisfy the following limits (Fig.3):

$$\lim_{h/R_i \rightarrow \infty} \beta = 1 \quad \text{and} \quad \lim_{h/R_i \rightarrow 0} \beta = 0 \quad (4)$$

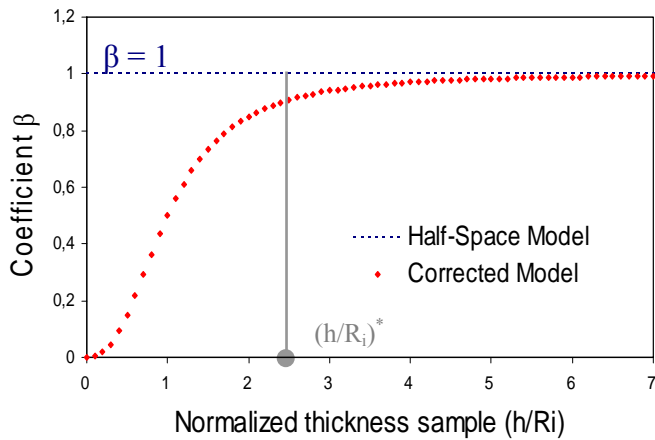


Fig.3: Comparison between half-space model of Theret & al. [3] and the corrected model. These simulations have been performed with $E = 1\text{kPa}$, $\nu = 0.49$, $\Delta P = 1\text{Pa}$ and $\eta = 0.4$. Notice that β is a constant equal to 1 for the half-space model.

3.5 Critical values of the sample thickness h

From the numerical results presented on Fig. 3, we derived the critical values of the ratio h/R_i , $(h/R_i)^*$, for which the relative error between the predictions of the half-space model and our corrected model (i.e. $(1-\beta)/\beta$) becomes smaller than 10%. We conclude that the influence of the tissue thickness must be considered as soon as the ratio h/R_i becomes smaller than 2.5.

Indeed, the relative error becomes larger than 20% for a sample thickness h smaller than the micropipette diameter $2R_i$ (Fig.3).

4 Conclusion

Estimation of the medium stiffness is a key issue for understanding how tissue reacts to an imposed stress. Considering the assumptions of quasi-incompressible elastic material undergoing small strains, our finite element computation indicates that below a critical value of h/R_i , the thickness of the sample becomes a relevant parameter and must be taken into account for accurately determining the mechanical properties of the tissue. If we use for experimental data analysis the Eq.(2) for thin tissue samples, the sample stiffness is overestimated. Therefore, this study provides a framework in which finite element modeling of biological tissue rheology would help to decrease the bias and thus the dispersion of elastic modulus estimated from micropipette experiments.

References:

- [1] O. Thoumine & al., Changes in the mechanical properties of fibroblasts during spreading: a micromanipulation study, *European Biophysics Journal*, 28, 1999, 222-234
- [2] A. A. Spector & al., Analysis of the micropipet experiment with the anisotropic outer hair cell wall, *Journal of the Acoustical Society of America*, 103, 1998, 1001-1006
- [3] D.P. Theret & al., The application of a homogeneous half-space model in the analysis of endothelial cell micropipette measurements, *Journal of Biomechanical Engineering*, 110, 1988, 190-199
- [4] MA. Haider & al., An axisymmetric boundary integral model for assessing elastic cell properties in the micropipette aspiration contact problem, *Journal of Biomechanical Engineering*, 124, 2002, 586-595
- [5] F. Guilak & al., Viscoelastic Properties of the Cell Nucleus, *Biochemical and Biophysical Research Communications*, 269, 2000, 781-786
- [6] T. Matsumoto & al., Local elastic modulus of atherosclerotic lesions of rabbit aortas measured by pipette aspiration method, *Physiological Measurement*, 23, 2002, 635-648.